Chapter 4
Cutting Under Gas Shields: Phenomenological Concepts Versus Industrial Applications

C.M.A. Silva, V.A.M. Cristino, P.A.R. Rosa and P.A.F. Martins

Abstract This chapter is focused on the interaction between cutting medium and freshly formed surfaces with the aim of providing a new level of understanding on the mechanics of chip flow in orthogonal metal cutting and analyzing its influence on the cutting forces and tool life in conventional milling. The first part of the chapter presents experimental results from an investigation performed with a specially-designed orthogonal metal cutting apparatus and a model material under dry conditions, with the objective of analyzing the influence of active and inert gas shields in the kinematics of chip flow, the friction coefficient, the chip-compression factor and the cutting forces. In particular, authors provide a correlation between surrounding medium, tribological conditions, surface roughness, freshly cut surfaces and chip curling at the tool-chip contact interface. The second part of the chapter extends the investigation to conventional milling of an engineering material in order to study the influence of cutting in the presence of air or under an argon atmosphere in the overall cutting forces and tool wear. Results from the investigation based on orthogonal metal cutting show that cutting in the presence of oxygen leads to higher values of friction, chip compression factor and chip curl radius, and to lower values of the shear plane angle. The presence of oxygen is also responsible for increasing the cutting forces and tool wear in conventional milling.

C.M.A. Silva · P.A.R. Rosa · P.A.F. Martins (✉)
Instituto Superior Técnico, Universidade de Lisboa,
Av. Rovisco Pais, 1049-001 Lisbon, Portugal
e-mail: pmartins@ist.utl.pt

C.M.A. Silva
e-mail: carlos.alves.silva@ist.utl.pt

P.A.R. Rosa
e-mail: pedro.rosa@ist.utl.pt

V.A.M. Cristino
Faculty of Science and Technology, University of Macau,
Av. Padre Tomás Pereira S.J., Taipa, Macau, China
e-mail: valentino.anok@ist.utl.pt

J.P. Davim (ed.), *Traditional Machining Processes*,
Materials Forming, Machining and Tribology, DOI 10.1007/978-3-662-45088-8_4

4.1 Introduction

Metal cutting plays a significant role in manufacturing due to its involvement either in the production of components or in the fabrication of tools and equipment utilized by other processes. Metal cutting, like in other metal working processes, is influenced by the tribological conditions at the tool-chip contact interface because they influence the way chip forms and curls, the heat and rise in temperature, the surface quality of the machined workpiece, the cutting forces, the energy requirements and the overall wear and life of the cutting tools.

Knowledge on the mechanics of chip flow has been driven by the study of metal cutting fundamentals, as reported in the state-of-the-art review paper by Jawahir and van Luttervelt [1]. The investigation started in the 1950s when chip curling was studied in connection with tool-chip contact length, restricted contact tools and clamped-on chip formers and, ever since then, there has been an enormous amount of research work in the area because the mechanics of chip flow is the basis for developing analytical and numerical models to predict cutting forces, chip curling, chip breaking, tool-wear and surface integrity.

Friction is also found to significantly influence the mechanics of chip flow. In fact, by reducing the friction coefficient, the shear plane angle ϕ increases, the chip thickness reduces and chip curling increases. Because the area of the shear plane decreases as well as the contact length and the applied pressure, the cutting force required for the process will decrease [2–4] (Fig. 4.1).

Despite the efforts performed by researchers over approximately 50 years, the explanation of how chips are formed, what is the role played by friction and what causes chips to curl are not yet clearly understood. Some of the most significant contributions in the field were systematized in Jawahir and van Luttervelt [1] and

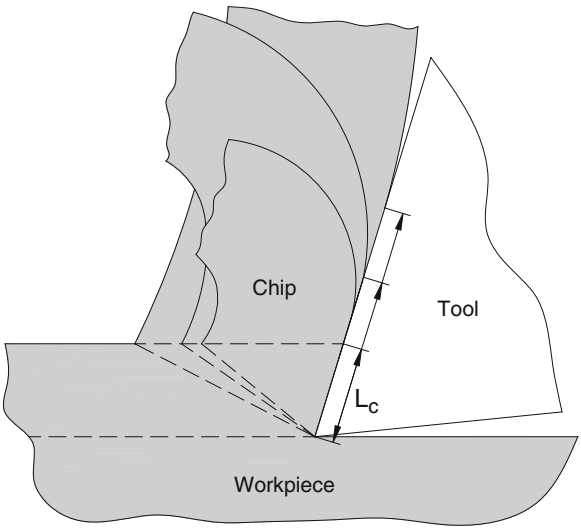

Fig. 4.1 Influence of the frictional conditions on the contact length and chip curling

van Luttervelt et al. [5] with the aim of saving fragmented and scattered experimental and theoretical knowledge in the mechanics of chip flow for further development.

The commonly accepted mechanism on chip formation in metal cutting consider that (i) new surfaces are formed by plastic flow around the tool edge, (ii) the energy required for cutting is overwhelmingly due to plasticity and friction and (iii) any energy required for the formation of new surfaces is negligible. This mechanism will be hereafter referred as the 'plasticity and friction only' view and is inherent in the most significant contributions to the understanding of metal cutting fundamentals made by Zorev [6], Shaw [7] and Oxley [8], among others (Fig. 4.2).

The primary shear zone, shown in Fig. 4.2a, extends from the cutting edge to the surface of the workpiece, and is the zone where the material is plastically deformed under high values of shear strains and stresses. The secondary shear zone occurs on the rake face of the cutting tool and results from plasticity and friction acting along

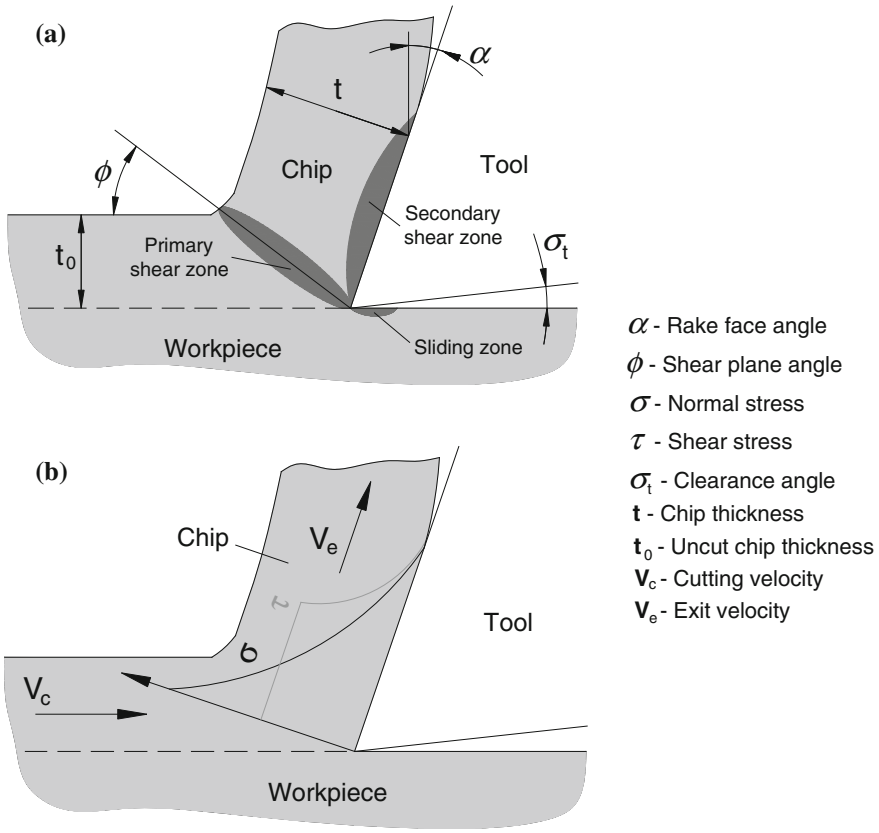

Fig. 4.2 Schematic representation of the commonly accepted chip formation mechanism with a basic set of notation that will be used throughout the chapter. **a** Representation of the zones of interest and **b** stress distribution proposed by Zorev [6]

the chip-tool contact interface. As originally developed by Zorev [6], the distribution of the normal and shear stresses on the rake surface gives rise to a region of seizure (or sticking) close to the cutting edge and to a region of sliding in the remaining contact interface (Fig. 4.2b).

The sliding zone along the clearance surface is caused by friction, increases with the area of contact between the tool and the workpiece, and is mainly responsible for producing flank wear in the cutting tools.

A recent breakthrough in the mechanics of chip formation was made by Atkins [9, 10] by extending traditional analysis to include the work involved in the formation of new surfaces at the tip of the tool (Fig. 4.3). The combination of plasticity and friction with ductile fracture mechanics proved effective for obtaining good estimates of the cutting forces and to solve a longstanding incompatibility problem of the metal cutting theory between the specific cutting pressure and the state-of-stress resulting from the stress-strain/strain rate behaviour of the materials [11].

In addition to what was mentioned previously, there is a common believe among researchers and practitioners that active gases (such as oxygen) acting on the freshly cut surfaces may influence friction, chip compression factor, chip curling and forces to a level that goes significantly beyond what has been said and written in the commonly accepted fundamentals of metal cutting. Despite early experiments conducted by Poletica (Astakhov [12]) on copper and armco iron, indicated that the surrounding medium does not show any influence, there is a necessity of revisiting the subject by identifying and quantifying the type of contaminant films as a function of the surrounding medium and the average surface roughness of the cutting tool.

Indeed, if the interaction between chip and tool in real metal cutting does not take into consideration the reactions of oxygen and nitrogen contained in the air with the freshly cut surfaces of the work material, there is room for misunderstanding the mechanics of chip flow and to consider curling solely as a consequence of static, kinematic and thermal effects caused by the operative cutting parameters. Not taking into account the extremely high sensitivity of metals to oxygen will also

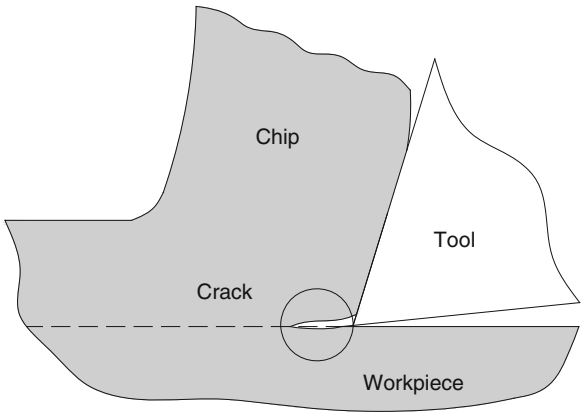

Fig. 4.3 Schematic representation of crack formation at the tip of the cutting tool

give rise to partial assessment of the role of cutting fluids and to erroneous estimates of the coefficient of friction along the rake surface of the cutting tools. This is probably one the main reasons why models for chip curling available in the literature are not widely applicable.

In fact, and in contrast to chip formation there has never been a universally accepted mechanism to explain what causes chips to curl. In general, results available in the literature estimate the radius of curvature to decrease with increasing depth of cut, with decreasing cutting velocity and decreasing friction and contact length at the rake face of the tool [1]. Some of these dependencies have been properly modelled by means of finite elements and artificial intelligence [5]. However, investigations by other authors also claim the distribution of stresses in the primary and secondary shear zones, thermal effects and work-hardening characteristics of the workpiece material to influence chip curl [13] and side-curl to be produced when machining dry and inhibited when using a lubricant [14].

This chapter is focused on the interaction between cutting medium and freshly formed surfaces with the aim of providing a new level of understanding on the mechanics of chip flow in orthogonal metal cutting.

The first part of the chapter presents thoroughly experimental results obtained from an investigation performed with a specially-designed orthogonal metal cutting apparatus and a model material under dry conditions, with the objective of analyzing the influence of active and inert gas shields in the kinematics of chip flow, the coefficient of friction, the chip-compression factor and the cutting forces. In particular, authors provide a correlation between surrounding medium, tribological conditions, surface roughness, freshly cut surfaces and chip curling at the tool-chip contact interface that may help assembling the puzzle of chip flow in metal cutting. The presentation enlarges previous published work in the field by the authors [15].

The second part of the chapter extends the investigation to conventional milling of an aluminium alloy AA7050-T7451 under industrial operating conditions. The choice of end milling was due to the fact that operating conditions and chip formation mechanisms differ considerably from those commonly found in steady-state orthogonal metal cutting. In fact, because the cutting edges of an end mill are at some angle of inclination to the direction of motion (oblique metal cutting), the cutting edges are not in constant contact with the workpiece surface and the undeformed chip thickness starts from zero and increases up to some maximum value determined by the chosen value of feed per cutting edge (or is thickest at engagement and tapers out to nothing in case of down or climb milling), it follows that the length of engagement for each cutting edge is short and the overall cutting time and exposure to oxygen for removing the same amount of material is larger than in orthogonal metal cutting. All this, combined with previous investigations by Yamane et al. [16] justify the importance for extending the work on the influence of cutting in the presence of air or under gas shields to conventional milling.

4.2 Orthogonal Metal Cutting Under Gas Shields

This section of the chapter is focused on the equipment, methods and procedures that were utilized for obtaining thoroughly researched results and proposing innovative explanations for the tribological conditions at the tool-chip contact interface that arise from the interaction between cutting medium, surface roughness and freshly cut metal surfaces in orthogonal metal cutting.

4.2.1 Equipment, Methods and Procedures

The experimental apparatus that was developed for performing orthogonal metal cutting under active and inert gas shields is schematically presented in Fig. 4.4, and is essentially composed by a cutting tool, a specimen, a nozzle, a three-dimensional piezoelectric dynamometer and a data acquisition system.

The cutting tool is mounted in the spindle and the specimen is fixed on the three-dimensional piezoelectric dynamometer, which is mounted directly on the work table of the machine. The experimental apparatus was installed in a Deckel-Maho DMC 63V machining center (Fig. 4.5).

The cutting tools were manufactured in AISI 316L stainless steel with a rake face angle $\alpha = 0°$, a clearance angle $\sigma = 0°$ and an edge radius below 2 μm (Fig. 4.6) for minimizing the contact with the clearance surface, where the arithmetical mean roughness R_a = 0.04 μm in order to ensure a smooth surface.

The surface texture, roughness and geometry of the cutting tools were carefully produced and regenerated in the Grinding and Polishing Unit (GPU) after completion of each test in order to ensure repeatability and analogy of surface topography irrespective of the test case. The GPU is schematically shown in Fig. 4.7 and consists in two separated blocks, each one for a respective tool's surface, with a well-defined geometry (rake and clearance angle) guarantying not only the reconditioning of the cutting tool, but also of the cutting edge sharpness.

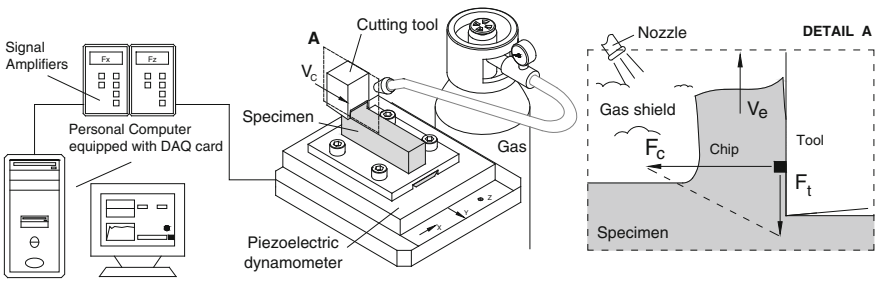

Fig. 4.4 Schematic representation of the experimental apparatus that was utilized in orthogonal metal cutting

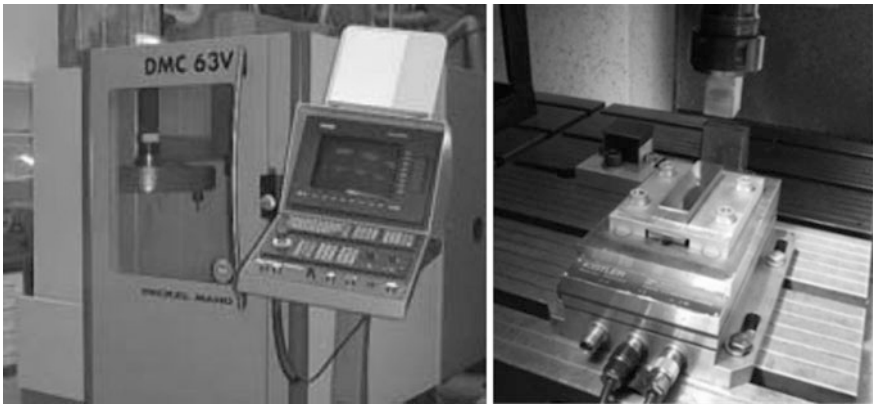

Fig. 4.5 The Deckel-Maho DMC 63V machining center with a detail of the experimental apparatus where the tests were performed

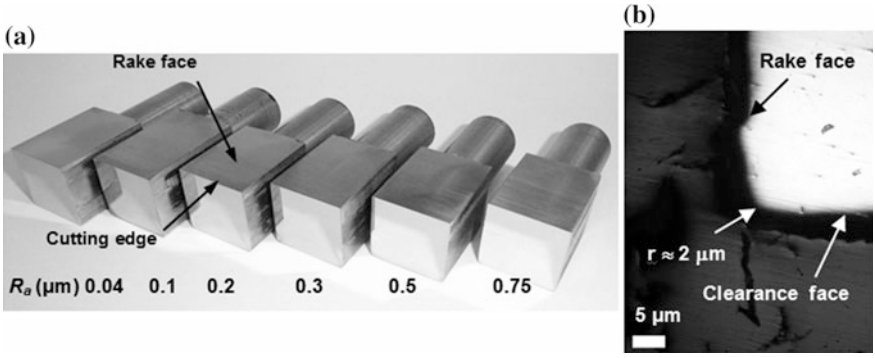

Fig. 4.6 **a** Cutting tools in AISI 316L stainless steel with different values of surface roughness and **b** detail of the tip of the tool showing the radius of the cutting edge

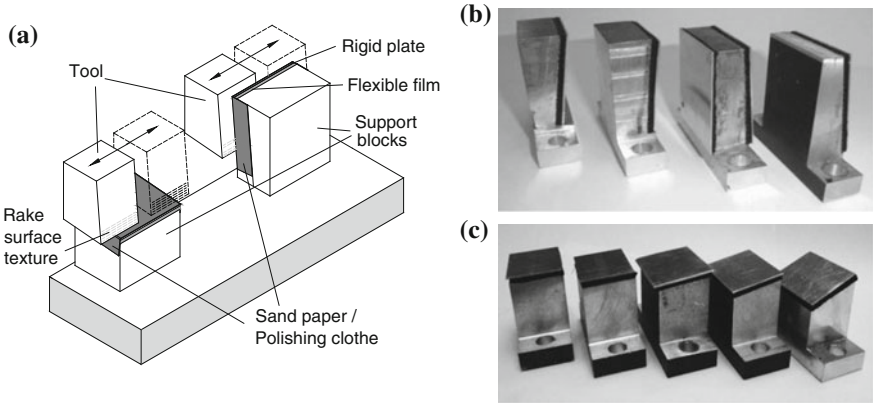

Fig. 4.7 **a** Schematic representation of the Grinding and Polishing Unit (GPU) and of the support blocks utilized for reconditioning the **b** rake and **c** clearance surfaces

The GPU is capable of providing average values of surface roughness (R_a) in the rake face within the range 0.04–0.75 μm. These values are measured by a roughness tester along the rake and relief surfaces of the cutting tool in a direction perpendicular to the cutting edge.

The specimens were made from technically-pure lead (99.9 %) with a rectangular cross section of 80 mm × 20 mm (length × width). The choice of technically-pure lead as a model material for the specimens was made in order to ensure narrow zones of intense plastic shearing under low cutting speeds, as required by the ideal orthogonal metal cutting conditions. This requirement is important for reducing the effect of strain-hardening, eliminating the influence of strain-rate sensitivity and keeping temperature rise, induced by energy dissipation due to plasticity and friction, low enough to allow the investigation to be exclusively focused on the influence of the surrounding medium in the mechanics of chip flow. The mechanical behaviour of technically-pure lead under low cutting speeds is not only capable of providing these operating conditions due to its near ideal rigid-plastic stress response as allows replicating the mechanical behaviour of conventional steels at the real manufacturing temperatures [17].

The influence of the surrounding medium was analysed by cutting in the presence of air and by shielding the cutting region by means of active and inert gases (oxygen, nitrogen or argon). The gases were supplied from an external source and applied at a rate of approximately 5 l/min through a nozzle to the cutting region (Fig. 4.4).

The three-dimensional piezoelectric dynamometer (Kistler 9257B) is attached to a signal amplifier (Kistler 5011B) and allows measuring the cutting forces during the tests (Figs. 4.4 and 4.5). The system is linear across its entire range, acquires forces with an accuracy of 1 % and its resolution allows measuring almost any dynamic changes in the forces of great amplitude. A personal computer data logging system based on a multifunction data acquisition card (National Instruments, PCI-6025E) combined with a special purpose LabView software controls testing, acquisition and storage of the experimental data.

Table 4.1 presents the experimental workplan for the entire set of test cases. The experiments were designed in order to correlate the influence of (i) gas shields

Table 4.1 The plan of experiments

Case	Uncut chip thickness t_0 (mm)	Cutting speed V_c (m/min)	Gas shield	Roughness R_a (μm)
1–6	0.2	0.6	Oxygen	0.04, 0.1, 0.25, 0.35, 0.45, 0.75
7–12	0.2	0.6	Nitrogen	0.04, 0.1, 0.25, 0.35, 0.45, 0.75
13–18	0.2	0.6	Air	0.04, 0.1, 0.25, 0.35, 0.45, 0.75
19–24	0.2	0.6	Argon	0.04, 0.1, 0.25, 0.35, 0.45, 0.75

(active vs. inert) and (ii) surface roughness of the cutting tools with chip curl radius, chip-compression factor, shear angle, friction coefficient and cutting and thrust forces. No lubricants were utilized during the tests.

Eliminating the influence of lubrication (dry cutting conditions), temperature and strain-hardening and maintaining the cutting speed (0.6 m/min) and the uncut chip thickness (0.2 mm) identical for all test cases revealed crucial for analysing the overall influence of active and inert gases on the mechanics of chip flow. The influence of size effects was also removed from experimentation because the ratio of the uncut chip thickness to the edge radius of the cutting tools was equal to 100. Otherwise, the number of possible combinations of variables and phenomena would become very large.

The experiments were done in a random order and several replicates were produced for each test configuration in order to provide statistical meaning.

4.2.2 Cutting and Thrust Forces

The experimental apparatus and the work plan described in the previous section allowed determining the cutting F_c and thrust F_t forces the entire set of test cases that are listed in Table 4.1. Figure 4.8 presents a typical evolution of these forces with time during an orthogonal metal cutting test performed in the presence of air.

As seen in the figure, the cutting and thrust forces increase sharply at the beginning of the test (refer to zone 'A' in Fig. 4.8) and remain almost constant throughout subsequent steady-state cutting conditions (refer to zone 'B' in Fig. 4.8). The sharp decrease in the evolution of the cutting and thrust forces with time that are observed in zone 'C' is not relevant for the overall discussion because it corresponds to unsteady-state cutting conditions that are typical of the end of the cutting test.

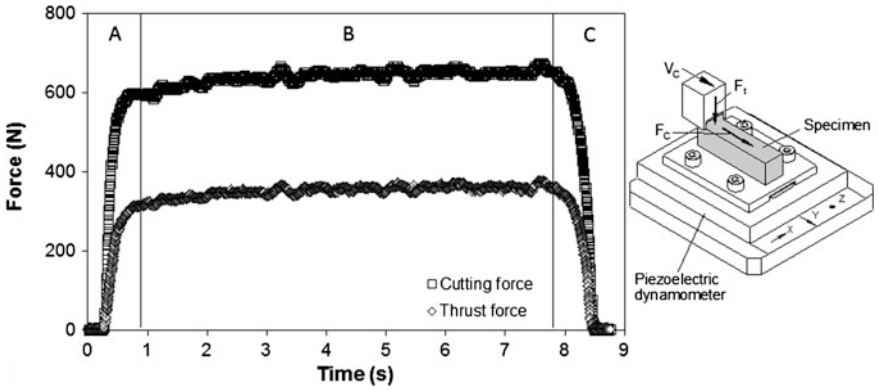

Fig. 4.8 Typical evolution of the cutting and thrust forces during an orthogonal cutting test performed in the presence of air ($\alpha = 0°$, $\sigma_t = 5°$, $R_a = 0.251$ µm, $t_0 = 0.2$ mm, $V_c = 0.6$ m/min)

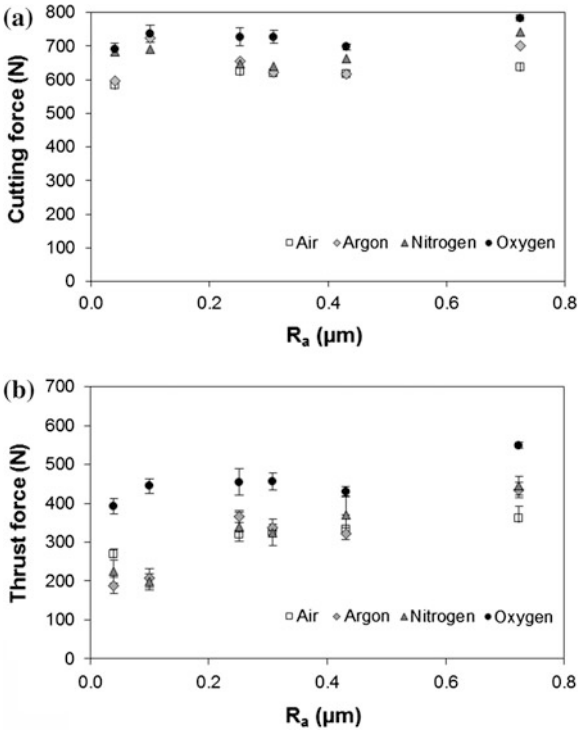

Fig. 4.9 **a** Cutting and **b** thrust forces as a function of surface roughness and surrounding medium

Figure 4.9 shows the experimental steady-state values of the cutting and thrust forces under different active and inert gas shields as a function of surface roughness for the entire set of test cases that are listed in Table 4.1.

As seen, dry cutting under an oxygen-rich atmosphere may require cutting and thrust forces up to 30 % higher than those needed in the presence of air or under an argon atmosphere. This is attributed to chemical reactions of oxygen with lead to form oxide films (PbO, the expected product of the chemical reaction between lead and oxygen) on the upper and lower surface boundaries of the chip and unveils the importance of the interactions between active gases and the freshly formed surfaces of the work materials.

Figure 4.9 also shows that cutting in the presence of air generally provides higher forces than those obtained under atmospheres of nitrogen or argon. This is because the low affinity of lead for nitrogen and the inert characteristics of argon avoid the formation of surface films on the freshly formed surfaces.

4.2.3 Friction Coefficient

The experimental values of the cutting F_c and thrust F_t forces that are acquired during the orthogonal metal cutting tests allow determining the friction coefficient.

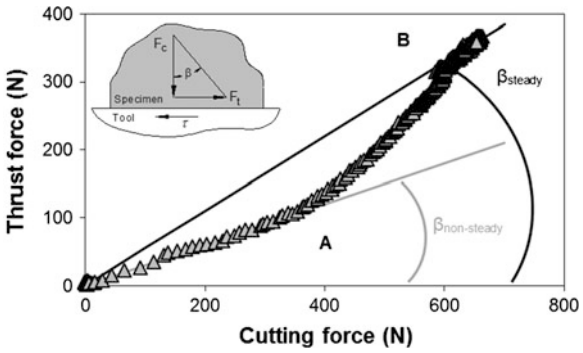

Fig. 4.10 Thrust force as a function of the cutting force during an orthogonal cutting test performed in the presence of air ($\alpha = 0°$, $\sigma_t = 5°$, $R_a = 0.251$ µm, $t_0 = 0.2$ mm, $V_c = 0.6$ m/min)

Considering, for example, the evolution of the forces with time that is plotted in Fig. 4.8 it is possible to produce a new graphic where the thrust force is plotted as a function of the cutting force that is relevant for the understanding and determination of the friction coefficient (Fig. 4.10).

As seen in Fig. 4.10 there are two different linear trends corresponding to values of the friction coefficient under non-steady state (regions 'A' in Figs. 4.8 and 4.10) and steady-state (regions 'B' in Figs. 4.8 and 4.10) cutting conditions. The friction coefficient is lower at the initial non-steady state conditions and higher at the steady-state cutting regime.

Similarly to what was previously done for the plot of the cutting and thrust forces as a function of surface roughness and surrounding medium, a similar procedure can be used for the friction coefficient $\mu = \tan \beta$ by taking into consideration the values of the friction coefficient μ_{steady} under steady-state conditions retrieved from the entire set of experimental tests that are listed in Table 4.1. The result is shown in Fig. 4.11 and allows identifying three different regions for the cutting tests

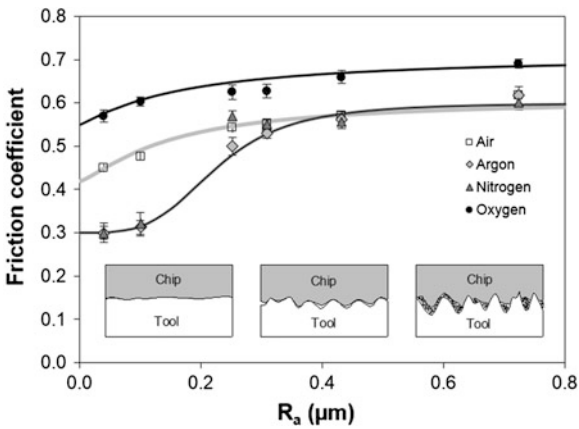

Fig. 4.11 Friction coefficient μ as a function of surface roughness R_a and surrounding medium

performed under nitrogen and argon gas shields: (i) a leftmost region ($R_a < 0.1$ μm) where the friction coefficient is constant and takes the smallest value among all the test cases, (ii) a rightmost region ($R_a > 0.3$ μm) where the friction coefficient is constant and takes the largest value among all the test cases and (iii) a region in-between where the friction coefficient progressively growths from the smallest to the largest measured values.

In the leftmost region of the graphics the basic source of friction is adhesion ($\mu \cong \mu_{adh}$) and the friction force resulting from the relative sliding movement between the chip and the cutting tool is roughly equal to the force that is needed for shearing the junctions formed by localized pressure welding (cold welding) at the asperities. This is because surface roughness is very small and because the low affinity of lead for nitrogen and the inert characteristics of argon avoid the formation of surface films, allowing the chip to slide smoothly along the rake surface of the cutting tool.

On the contrary, in the rightmost region of the graphic (where surface roughness of the cutting tool is very large) there is a more pronounced interaction between the asperities namely, the penetration and plastic deformation of the boundary surfaces of the chips and, in some cases, the formation of debris from micro-cutting at the asperity level (refer to the rightmost inset detail in Fig. 4.11). The increase of ploughing and the extra resistance to sliding caused by loose debris raise the friction force and, therefore, the friction coefficient for rougher tools is larger than for smoother tools.

The results obtained from the orthogonal cutting tests in the presence of air or under an oxygen-rich atmosphere do not show evidence of the aforementioned first and second regions of the graphic (Fig. 4.11) because both cases show a monotonic increase of the friction coefficient from smaller to larger values of surface roughness. This is attributed to the oxide films of PbO formed in the upper and lower surface boundaries of the chips, which do not allow material to slide smoothly along the rake surface of the cutting tools, even when roughness is very small. Finally, it is worth notice that the affinity of lead for oxygen is responsible for increasing the overall level of friction even when cutting with tools having large surface roughness.

4.2.4 Chip Curling

Although the influence of the surrounding medium in metal cutting is often resumed to its primary function of cooling and lubricating, one important aspect of the cutting medium on the tribological conditions at the tool-chip contact interface is the protection against active gases in air.

Figure 4.12a presents the cross section of the chips obtained for the entire test cases that are listed on Table 4.1. As seen, cutting under nitrogen or argon atmospheres allow chips to curl naturally within the normal range of surface roughness currently found in cutting tools whereas the exposure to oxygen causes the chip curl

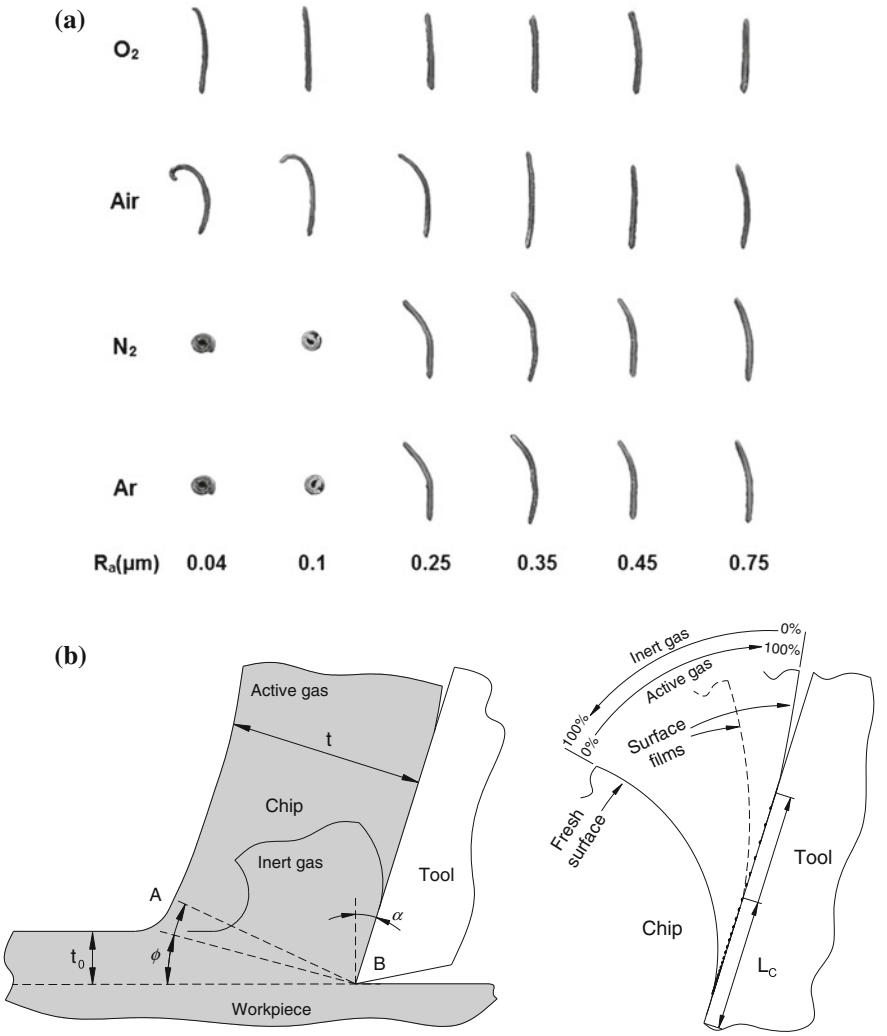

Fig. 4.12 **a** Pictures of chip cross sections obtained in cutting tests performed under different surface roughness and surrounding medium conditions, and **b** schematic representation of chip flow as a function of the surrounding medium

radius to become larger. In fact, the exposure to oxygen causes the chips to flow along the rake surface of the cutting tools, increasing the contact length L_c (Fig. 4.12b), and promoting its curvature away from the cutting edge.

The contact length L_c in steady-state cutting conditions is due to an energy compromise between the plastic work, a quantity inversely proportional to the radius of curvature of the chip, and the amount of frictional work which is directly proportional to the contact length and, therefore, to the radius of curvature of the chip. Because, cutting in the presence of oxygen increases the friction coefficient

(Fig. 4.11), it follows that frictional work will also increase with the formation of oxide films on the new freshly cut surfaces of lead. The exposure of lead to oxygen also results in larger chip curl radius (Fig. 4.12a).

The influence of the surrounding medium in the mechanics of chip flow can be further understood by analysing the evolution of the chip compression factor t/t_0 and of the primary shear plane angle ϕ as a function surface roughness R_a for cutting tests performed in the presence of different gas shields (Fig. 4.13):

$$\frac{t}{t_0} = \frac{\overline{AB} \cdot \cos(\phi - \alpha)}{\overline{AB} \cdot \sin \phi} = \cot \phi \cos \alpha + \sin \alpha \tag{4.1}$$

where α is the rake angle, t_0 the uncut chip thickness and t the chip thickness.

Two different patterns of behaviour can be distinguished; in case of inert gas shields the chip compression factor t/t_0 and the primary shear plane angle ϕ are very sensitive to the surface roughness R_a whereas in case of cutting in the presence of active gases the aforementioned sensitivity is less important.

In the first pattern type of behaviour, chip thickness decreases (using the original uncut chip thickness as reference) as surface roughness R_a diminishes due to an increase of the shear plane angle ϕ. As a result of this, the contact length L_c at the

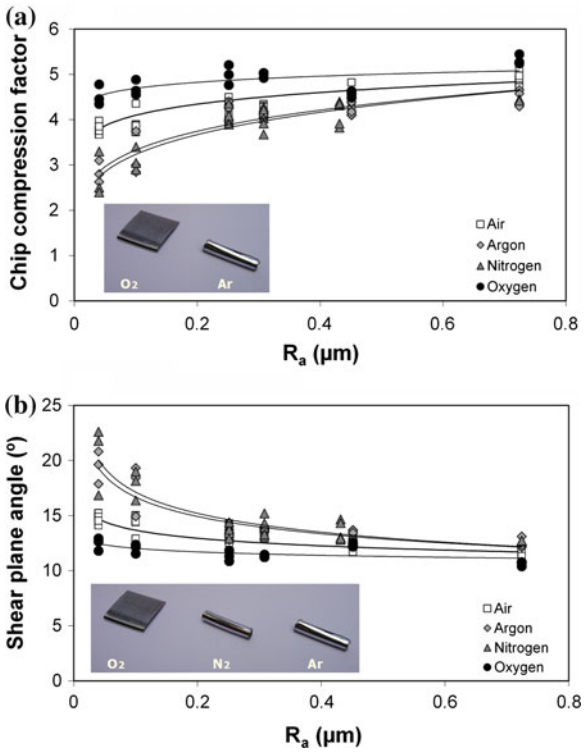

Fig. 4.13 **a** Chip compression factor and **b** shear plane angle as a function of surface roughness and surrounding medium. *Insets* show pictures of chips produced by cutting in the presence of different gas shields

rake tool surface is diminished and curling of the chip is promoted when cutting in the presence of argon and nitrogen, as shown in the photographs included in Fig. 4.13.

The second pattern type of behaviour in Fig. 4.13 is similar to that of cutting under dry conditions. The curling radius is much larger than that experimentally observed in case of cutting in the presence of inert gas shields and the acquired data points towards the influence of oxide films of PbO to be more important than the diminishing the surface roughness R_a. As expected, the influence of oxide films in the mechanics of chip flow reaches a maximum when cutting in the presence of an oxygen gas shield.

The influence of surface roughness in chip curling can be further analysed in Fig. 4.12. As seen, the higher the roughness, the smaller is the influence of the surrounding medium and the greater are the difficulties for the chips to curl away from the rake face. This is due to a more pronounced interaction between the asperities of the chip and tool and allows us to conclude that cutting in the presence of active gases will diminish the magnitude of the shear plane angle ϕ and will produce thicker chips than in case of cutting under low-affinity or inert atmospheres.

The results supporting these conclusions are in line with common believes among researchers and practitioners that oxygen may significantly influence the mechanics of chip flow and go against published research work in the field claiming no influence of the surrounding medium, that was referred in the introduction to this chapter.

The proposed mechanism for explaining the influence of oxygen in the mechanics of chip flow is shown in Fig. 4.14 and requires contact length L_c to be divided into three main regions; (i) the bottom newly cut surface of the chip (denoted as '1' in Fig. 4.14a), (ii) the intermediate surface of the chip (2) and (iii) the upper surface (3) that extends up to the point where chip separates from tool.

Region '1' is in immediate and intimate contact with the rake face of the tool, is submitted to high normal pressures and is uncontaminated by oxygen. Because its length is small (approximately or slightly greater than t_0) and its roughness R_a is also small the basic source of friction in region '1' is expected to be adhesion.

Region '2' experiences less significant normal pressures than previous region '1' but its exposure to oxygen results in the formation of oxide films in the lower surface boundary of the chip. Figure 4.14a, b show a schematic representation and a photograph of the oxide films that were formed on the surface boundary of the chip and were subsequently smeared over the rake face of the tool (refer to the light coloured strips in Fig. 4.14a) when cutting in the presence of air or under an oxygen-rich atmosphere. Because the average thickness of the oxide films was found to be 3 μm, which is a value significantly larger than the average surface roughness of the rake face of the cutting tool, it is possible to conclude that the interaction between cutting medium and freshly formed surfaces is strong and penetrates deep into the metallic substrate. It is worth notice that in case of cutting under nitrogen or argon atmospheres there is no evidence of surface films left on the

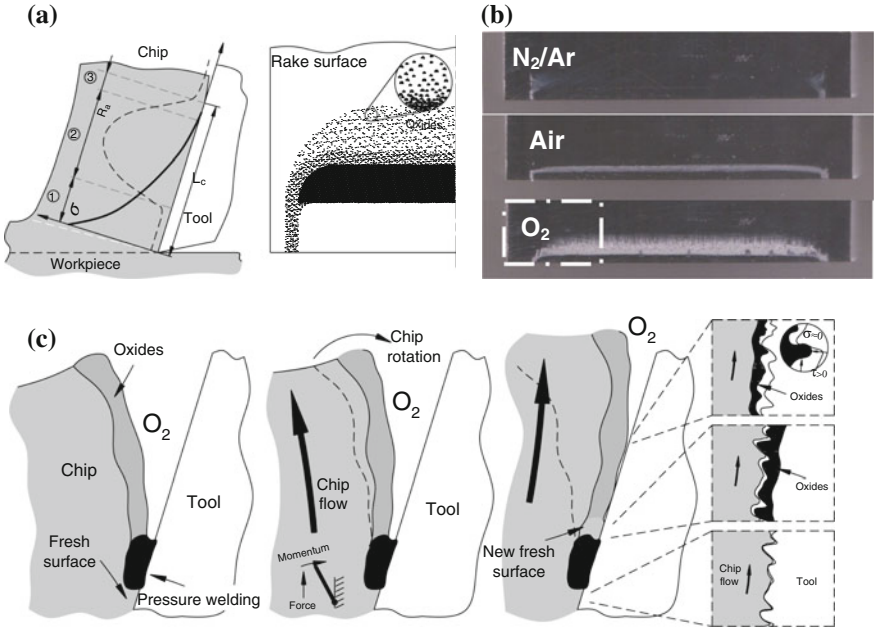

Fig. 4.14 Cutting under inert and active gas shields: **a** schematic representation of the oxide films that were formed on the freshly cut surface of the chip and are pressure welded onto the rake face of the cutting tool, **b** photographs showing evidence of oxide films on the tool rake face when cutting in the presence of air or under an oxygen gas shield and **c** the proposed mechanism for explaining the influence of oxide films in chip curl

rake face of the tool (Fig. 4.14b) and, therefore, roughness after cutting is similar to that before cutting.

As seen, the oxide films that are pressure welded onto the rake face of the cutting tool are spread throughout a larger area in case of cutting under an oxygen-rich atmosphere than in the presence of air. The increase in surface roughness due to the oxides (Fig. 4.14) in conjunction with the extra force that is needed for shearing the junctions formed between the oxide particles and the asperities gives rise to higher values of friction in region '2'. Material flow behaviour approaches sticking conditions, due to a more pronounced interaction between the oxide particles and the asperities and this creates difficulties for the chips to curl away from the rake face of the cutting tools, thereby, increasing its overall contact length L_c (Fig. 4.14c). This explains the differences observed in the chip cross sections that are pictured in Fig. 4.12.

Region '3' experiences the lowest normal pressures. Scattered oxide films, if present, are likely washed away during sliding of the chip along the rake face of the cutting tools and this explains the reason why Fig. 4.14b shows no signs of contamination arising from the lower surface boundaries of the chips.

The above conclusion helps clarifying the role of cutting fluids in metal cutting. In fact, besides cooling the working area, thereby reducing its temperature, distortion and improving tool life, cutting fluids are also responsible for protecting the freshly formed surfaces of the work material from active gases such as oxygen.

4.3 Milling Under Gas Shields

This last section of the chapter extends the investigation to conventional milling of an engineering material and is exclusively focused on the influence of the surrounding medium in the cutting forces and tool wear.

4.3.1 Equipment, Methods and Procedures

The experimental apparatus that was developed by the authors to perform conventional milling tests under gas shields is schematically presented in Fig. 4.15a and is essentially composed by a cutting tool, a specimen, a gas chamber, a three-dimensional piezoelectric dynamometer, a data acquisition system and a confocal chromatic imaging measurement system (Fig. 4.15d).

The cutting tool is a solid end mill cutter JS513(51) supplied by Seco Tools with three cutting edges, 16 mm diameter, an helix angle of 20° and a corner radius equal to 0.16 mm (Fig. 4.15b). The selection of an end mill with three cutting edges provides a good compromise between end mills with two cutting edges that have better space for chip ejection and end mills with four cutting edges that ensure better surface finishes. The utilization of a heat shrink tool holder, in which the tool holder clamping area is heated for a few seconds before inserting the end mill cutter, ensures excellent rigidity and concentricity of the end mill with tool run-outs below 2 μm.

The specimens were made from aluminium AA7050-T7451 with a rectangular cross section of 140 × 100 (length × width). This choice of material served the dual purpose of carrying out the investigation in an engineering material (widely used in the aerospace industry) and selecting a material with high affinity to oxygen. The affinity of aluminium to oxygen is responsible for the formation of a surface layer of alumina (or, aluminium oxide) Al_2O_3 of approximately 1 μm thickness with high hardness and abrasivity.

The cutting parameters employed in the milling tests are summarized in Table 4.2. All tests were performed in dry conditions, in the presence of air or under an argon atmosphere, in end milling conditions. The choice of parameters was performed with the objective of increasing tool wear, reducing the influence of temperature in chip formation and eliminating any extra influence of oxygen beyond that arising from cutting in the presence of air that would result from

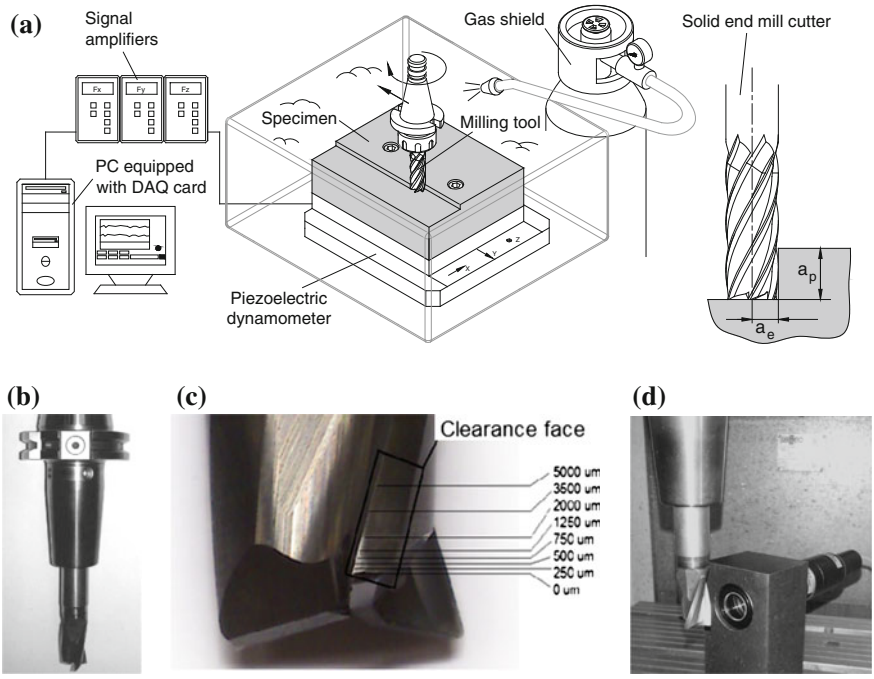

Fig. 4.15 Milling under gas shields. **a** Schematic representation of the experimental apparatus that was utilized in the tests, **b** the end mill and the heat shrink tool holder, **c** wear measuring locations with reference to distances to the end cutting edge **d** picture of the confocal chromatic imaging measurement system that was utilized for measuring tool wear

Table 4.2 The cutting parameters for the milling tests

Depth of cut, a_p (mm)	2
Width of cut, a_e (mm)	2
Cutting speed, V_c (m/min)	300
Feed rate, f (mm/min)	600
Feed per tooth, f_z (mm)	0.033

dissociation of water molecules into oxygen and hydrogen, if cutting fluid emulsions were employed.

The cutting forces were measured by means of a three-dimensional piezoelectric dynamometer (Kistler 9257B) attached to a signal amplifier (Kistler 5011B). A personal computer data logging system based on a multifunction data acquisition card (National Instruments, PCI-6025E) combined with a special purpose LabView software was employed for the acquisition and treatment of the experimental data.

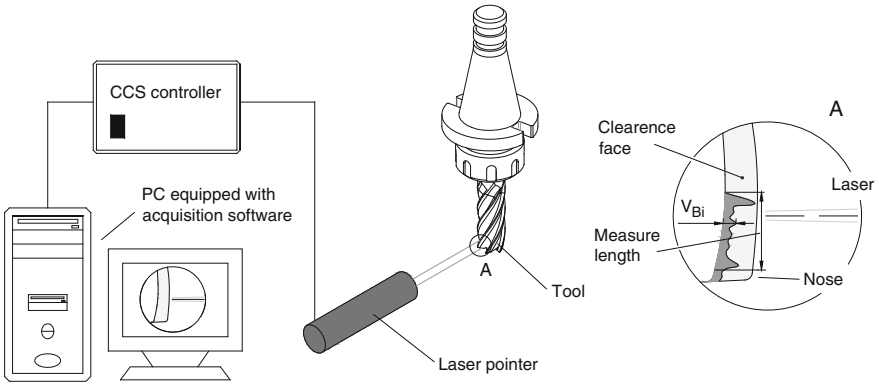

Fig. 4.16 Schematic representation of the experimental set up that was utilized for measuring tool wear in the milling tests

In general, tool wear can take several forms such as flank wear, notch wear, crater wear, edge rounding and edge cracking, among others. All these wear mechanisms play a role in tool life, which is usually characterized by the maximum number of machined parts or the maximum duration (for example, in hours) of operation it takes to reach a specific condition (or criterion).

This section of the chapter is focused on tool wear caused by the intense rubbing of the clearance faces of the milling tool over the freshly formed surfaces of the specimen. This type of wear is commonly designated as 'flank wear' and leads to the formation of a wear land.

The width V_B of the wear land was measured by means of a confocal chromatic laser based imaging system (Fig. 4.15d) that employs a white light confocal displacement sensor CL4-MG35 and a controller STIL Initial 4.0 with a resolution of 130 nm and a precision of 300 nm (Fig. 4.15d). The equipment and procedure is schematically shown in Fig. 4.16 and the measuring locations were performed with reference to distances of 250, 500, 750 and 1,250 μm to the end cutting edge (Fig. 4.15c).

The overall experimental apparatus for performing the milling tests was installed in the Deckel-Maho DMC 63V machining center that had been previously utilized in the orthogonal metal cutting tests (refer to Fig. 4.5).

4.3.2 Cutting Forces

Figure 4.17a shows the experimental cutting forces F_x, F_y and F_z measured by means of the three-dimensional piezoelectric dynamometer during one turn performed after 25 h of milling under dry conditions in the presence of air.

The three peaks with increasing amplitudes of the experimental cutting force F_y that are denoted as 'A', 'B' and 'C' in Fig. 4.17a are associated with the three

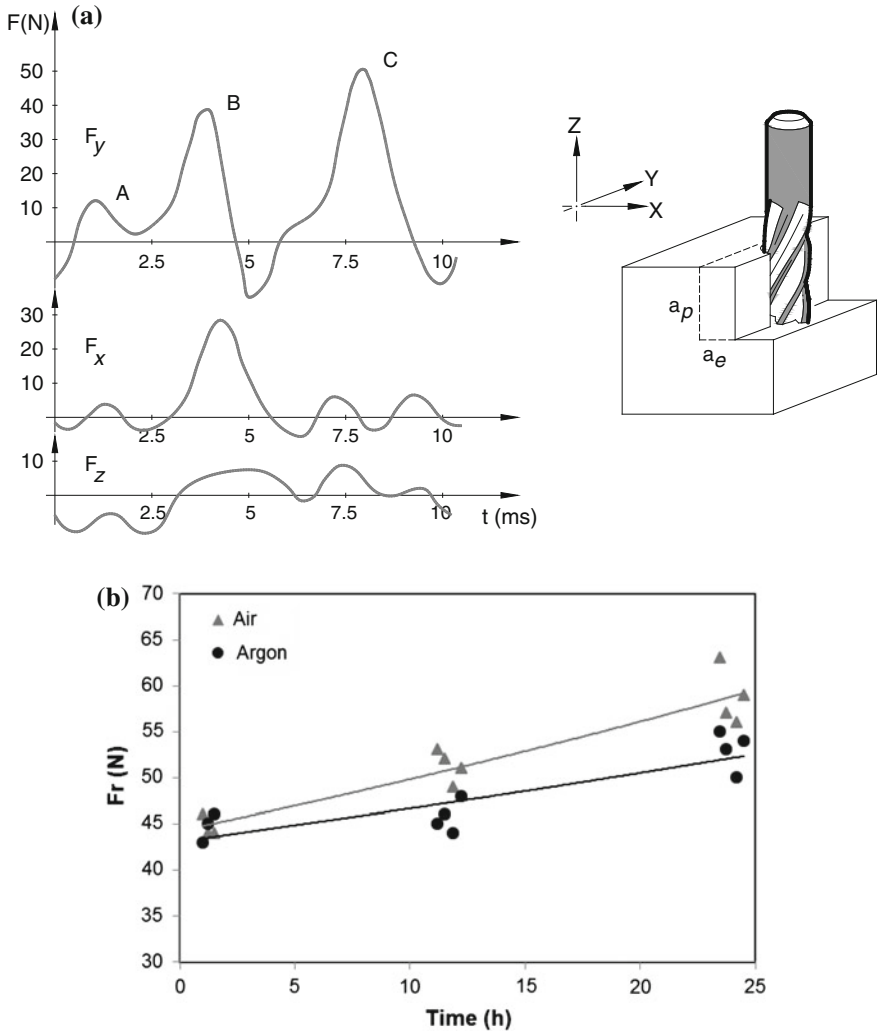

Fig. 4.17 **a** Three-dimensional cutting forces after 25 h of milling under dry conditions in the presence of air and **b** resultant force F_r in the xy-plane as a function of the milling time and the surrounding medium

different cutting edges of the end mill. The evolution of the cutting forces F_x, F_y and F_z during the 10 ms that are needed for the end mill to complete a full turn allow concluding that the third cutting edge, corresponding to a maximum peak force $F_y = 50$ N (obtained after 7.5 ms—refer to 'C'), is the outermost cutting edge of the tool. Moreover, results also show that the instant of time where the maximum peak force 'C' is registered is approximately coincident with the instant of time when the

cutting velocity is aligned with the y-axis of the piezoelectric dynamometer ($F_x \cong 0$ N).

The negative values of the cutting force F_y are caused by the ejection of chips along the y-axis.

By performing the acquisition of the experimental cutting forces in two other instants of time corresponding to 1 and 24 h of operation and plotting the resultant force F_r (in the xy-plane),

$$F_r = \sqrt{F_x^2 + F_y^2} \tag{4.2}$$

as a function of time and surrounding medium (Fig. 4.17b), it is possible to conclude that major differences derived from milling in the presence of air or under an argon atmosphere are only noteworthy above 10 h of operation. In fact, only after 10 h of operation the resultant force F_r experiences a faster growth with time when milling in the presence of air than under an argon atmosphere.

4.3.3 Tool Wear

Figure 4.18 presents a schematic representation of tool wear in a solid end mill cutter with three cutting edges. Wear occurs simultaneously in the rake and clearance faces and gives rise to a reduction $2 \times \Delta R_t$ in the diameter of the end mill and to an increase of the contact width V_{Bi} between the clearance face and the workpiece. Figure 4.19 shows the evolution of the reduction in the radius of the end mill with the milling time and the surrounding medium.

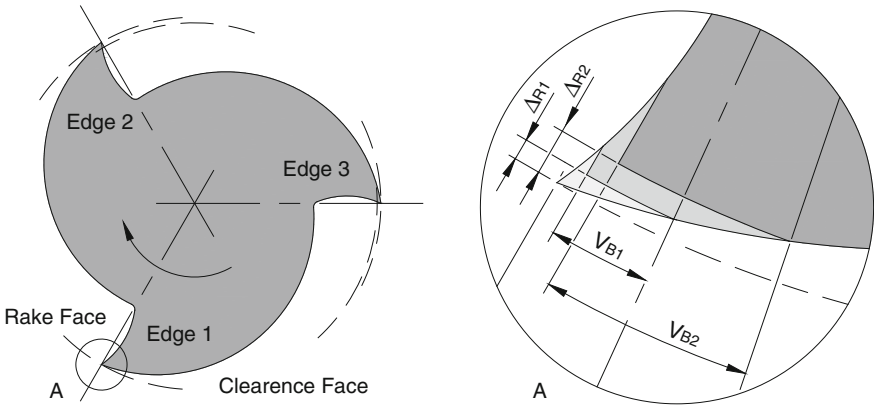

Fig. 4.18 Schematic representations of tool wear in a solid end mill cutter with three cutting edges with the dimensions that are utilized for its characterization

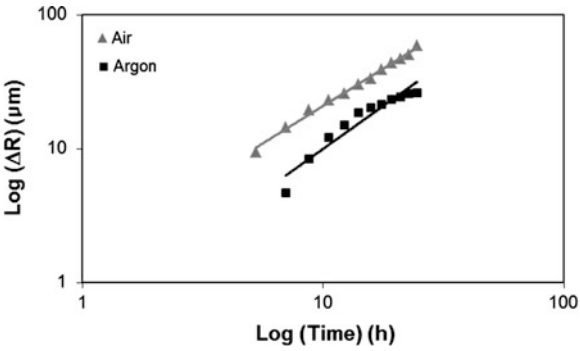

Fig. 4.19 Reduction in the radius of the end mill as a function of the milling time and surrounding medium

Tool wear in the rake and clearance faces are caused by abrasive and adhesive mechanisms resulting from the affinity of the fleshly formed surfaces to oxygen. They are the most common wear modes in conventional milling and are generally undesirable because dimensional control of the workpiece is lost, surface finished deteriorates and heat generation increases.

Figure 4.20a shows the widths V_{Bi} of the flank wear land after t_i hours of milling that were measured by means of the confocal chromatic imaging system at locations corresponding to 250, 500, 750 and 1,250 μm distance from the end cutting edge. As seen, after the initial 3–5 h of operation wear starts growing rapidly, between 10 and 20 h of operation wear settles down to a nearly steady-state rate, and after 20 h of operation wear accelerates once again towards the end of tool life.

Results in Fig. 4.20a also show that cutting in the presence of air accelerates flank wear, thereby, reducing tool life. In fact, milling under an argon atmosphere allows reducing flank wear by approximately 50 % in 25 h of operation. This result is in good agreement with those obtained by other researchers [16].

The abovementioned evolution of the flank wear with the milling time and surrounding medium for a particular cutting edge can be extrapolated to the other two cutting edges, placed in different radial positions, as proved by the linear interpolation (with a slope equal to 1.01) that is presented in Fig. 4.20b.

The increase of tool life by cutting in the presence of an argon atmosphere may be explained by the prevention of alumina Al_2O_3 formation at the contact interface between the cutting edges and the fleshly formed surfaces of the workpiece and also by its avoidance during the period of time when the surfaces are not in contact with the cutting edges. The latter is very important because it prevents the cutting edges from engaging the hard and abrasive surface layer of alumina each time a new cut starts. Instead, the cutting edges will always engage the more ductile and less abrasive aluminium alloy.

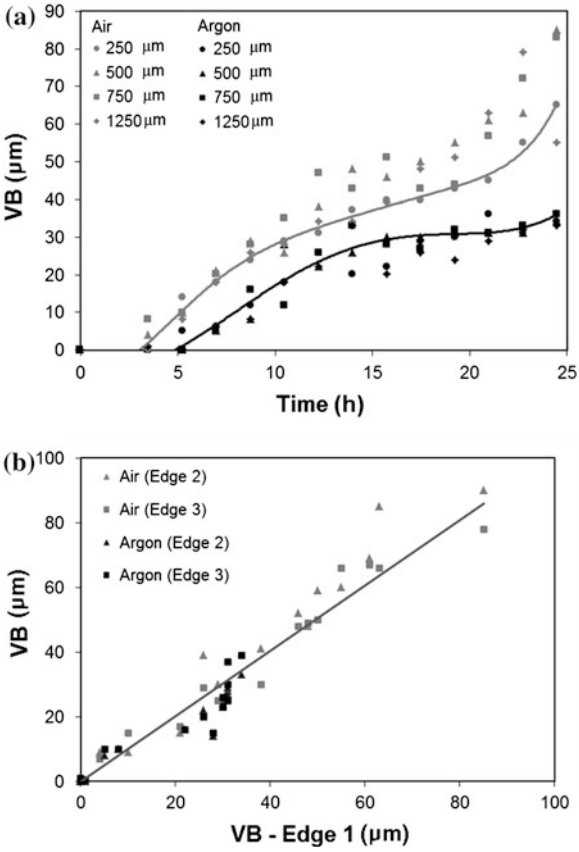

Fig. 4.20 **a** Flank wear in a cutting edge as a function of the milling time and surrounding medium and **b** Flank wear in cutting edges 2 and 3 as a function of the flank wear in cutting edge 1 (values measured at 500 µm distance from the end cutting edge)

4.4 Conclusions

This chapter presented the influence of the surrounding medium in the mechanics of chip flow by performing orthogonal metal cutting and conventional milling under active and inert gas shields. The experimental results obtained from orthogonal metal cutting show that cutting in the presence of oxygen leads to higher values of friction, chip compression factor and chip curl radius and to lower values of the shear plane angle. This indicates that the surface films formed on a freshly cut surface will significantly influence the mechanics of chip flow.

The proposed model for explaining the influence of surface films on the mechanics of chip flow during orthogonal metal cutting that is based on the interaction between chip and tool rake face, allows understanding the reason why cutting in the presence of oxygen will increase the contact length and promote curvature away from the cutting edge.

Similar results obtained in conventional milling of an aluminium alloy allow concluding that oxygen has a significant influence on the overall cutting conditions, namely in the increase of the cutting forces and tool wear.

All these results point towards the importance of taking the interaction between the cutting tools and freshly formed surfaces into account due to chemical reactions with active gases in the atmospheric air. In fact, not taking this interaction into consideration leads to misunderstanding of the mechanics of chip flow, the sources of friction along the rake surface of the cutting tools, the cutting forces, the tool wear and the role of cutting fluids, when used.

Acknowledgments The authors would like to acknowledge the support provided by Embraer, Portugal.

References

1. Jawahir IS, van Luttervelt CA (1993) Recent developments in chip control research and applications. Ann CIRP 42:659–693
2. Nakayama K, Ogawa M (1978) Basic rules on form of chip in metal cutting. Ann CIRP 27 (1):17–21
3. Kluft W, Konig W, Luthukelt CA, Nakayama K, Pekelkuing AJ (1979) Present knowledge of chip control. Ann CIRP 28/2:441–455
4. Pekelharing AJ (1963) Why and how does the chip curl and break. Ann CIRP 12(1):144–147
5. van Luttervelt CA, Childs THC, Jawahir IS, Klocke F, Venuvinod PK (1998) Present situation and future trends in modelling of machining operations—progress report of the CIRP working group 'modelling of machining operations'. Ann CIRP 47:587–626
6. Zorev N (1966) Metal cutting mechanics. Pergamon Press, Oxford
7. Shaw MC (1984) Metal cutting principles. Clarendon Press, Oxford
8. Oxley PLB (1989) Mechanics of machining: an analytical approach to assessing machinability. Wiley, New York
9. Atkins AG (2003) Modelling metal cutting using modern ductile fracture mechanics: quantitative explanations for some longstanding problems. Int J Mech Sci 45:373–396
10. Atkins AG (2009) The science and engineering of cutting. Butterworth-Heinemann, Oxford
11. Rosa PAR, Martins PAF, Atkins AG (2007) Revisiting the fundamentals of metal cutting by means of finite elements and ductile fracture mechanics. Int J Mach Tools Manuf 47:607–617
12. Astakhov VP (2006) Tribology of metal cutting. Elsevier, Oxford
13. Kalpakjian S (1997) Manufacturing processes for engineering materials. Addison-Wesley, Reading
14. de Chiffre L (1990) Metal cutting mechanics and applications. DSc. thesis, Technical University of Denmark
15. Cristino VAM, Rosa PAR, Martins PAF (2010) Cutting under active and inert gas shields: a contribution to the mechanics of chip flow. Int J Mach Tools Manuf 50:892–900
16. Yamane Y, Narutaki N, Hayashi K (1996) Suppression of tool wear by using an inert gas in face milling. J Mater Process Technol 62:380–383
17. Altan T, Henning HJ, Sabroff AM (1970) The use of model materials in predicting forming loads in metalworking. J Eng Ind Trans ASME 92:444–452